Cell Reports
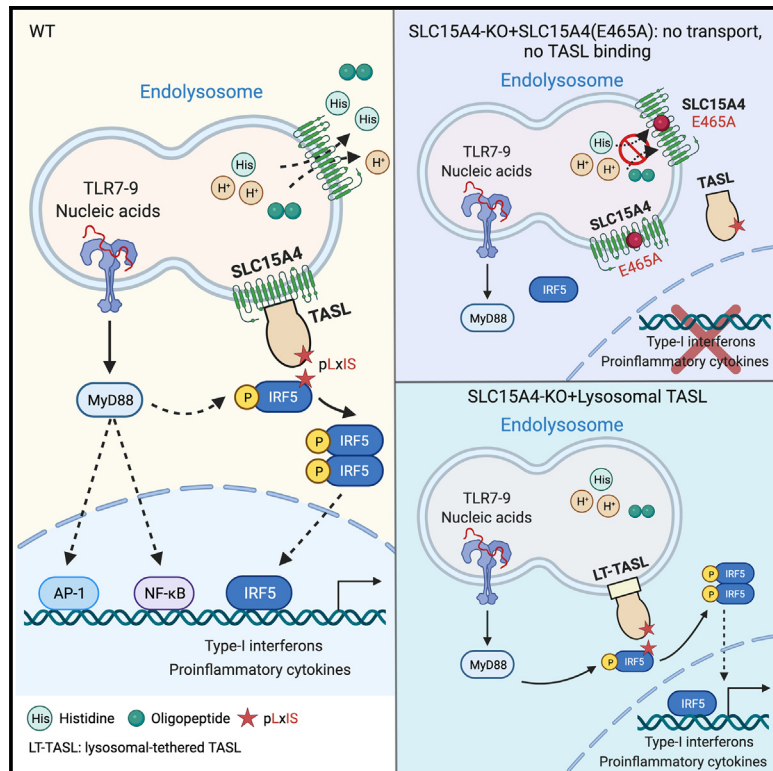
SLC15A4 controls endolysosomal TLR7–9 responses by recruiting the innate immune adaptor TASL

Graphical abstract

Authors
Haobo Zhang, Léa Bernaleau,
Maeva Delacrétaz, Ed Hasanovic,
Ales Drobek, Hermann Eibel,
Manuele Rebsamen

Correspondence
manuele.rebsamen@unil.ch

In brief

Zhang et al. show that the crucial function of lupus-associated solute carrier 15A4 in TLR7–9 responses is to act as a signaling hub recruiting TASL to endolysosomes. SLC15A4 transport activity is dispensable when TASL is tethered to this compartment. Targeting TASL to endolysosomes restores TLR7–9-dependent responses in SLC15A4-deficient cells.

Highlights

- Fusion of TASL to transport-deficient SLC15A4 rescues TLR7–9 responses

- Endolysosomal-tethered TASL restores TLR7–9 signaling in SLC15A4-deficient cells

- The SLC15A4-TASL complex is required for TLR7–9-induced IRF5 in human B cells

- The role of SLC15A4 in TLR7–9 pathways is to act as a scaffold for TASL recruitment

CellPress

Report

SLC15A4 controls endolysosomal TLR7–9 responses by recruiting the innate immune adaptor TASL

Haobo Zhang,[1] Léa Bernaleau,[1] Maeva Delacrétaz,[1] Ed Hasanovic,[1] Ales Drobek,[1] Hermann Eibel,[2,3] and Manuele Rebsamen[1,4,*]

[1]Department of Immunobiology, University of Lausanne, Ch. des Boveresses 155, 1066 Epalinges, Switzerland
[2]Department of Rheumatology and Clinical Immunology, Medical Center and Faculty of Medicine, University of Freiburg, Hugstetterstr. 55, 79106 Freiburg, Germany
[3]Center for Chronic Immunodeficiency, Medical Center and Faculty of Medicine, University of Freiburg, Breisacherstr. 115, 79106 Freiburg, Germany
[4]Lead contact
*Correspondence: manuele.rebsamen@unil.ch
https://doi.org/10.1016/j.celrep.2023.112916

SUMMARY

Endolysosomal Toll-like receptors (TLRs) play crucial roles in immune responses to pathogens, while aberrant activation of these pathways is associated with autoimmune diseases, including systemic lupus erythematosus (SLE). The endolysosomal solute carrier family 15 member 4 (SLC15A4) is required for TLR7/8/9-induced responses and disease development in SLE models. SLC15A4 has been proposed to affect TLR7–9 activation through its transport activity, as well as by assembling an IRF5-activating complex with TASL, but the relative contribution of these functions remains unclear. Here, we show that the essential role of SLC15A4 is to recruit TASL to endolysosomes, while its transport activity is dispensable when TASL is tethered to this compartment. Endolysosomal-localized TASL rescues TLR7–9-induced IRF5 activation as well as interferon β and cytokine production in SLC15A4-deficient cells. SLC15A4 acts as signaling scaffold, and this function is essential to control TLR7–9-mediated inflammatory responses. These findings support targeting the SLC15A4-TASL complex as a potential therapeutic strategy for SLE and related diseases.

INTRODUCTION

Detection of invading pathogens by the innate immune system is central to mount protective responses.[1] Microbial-derived nucleic acids are recognized by both cytosolic sensors as well as endolysosomal transmembrane Toll-like receptors (TLR) 3, 7, 8, and 9.[2–5] These innate immune pathways play a critical role to control viral and bacterial infections by inducing antimicrobial genes, triggering the production of interferons and proinflammatory cytokines and priming tailored adaptive immune responses. Conversely, aberrant activation of nucleic acid-sensing pathways is involved in a broad spectrum of pathologies, ranging from interferonopathies to autoimmune conditions such as systemic lupus erythematosus (SLE).[6–8]

A central pathogenic event in SLE and closely related autoimmune diseases is the engagement of endolysosomal TLRs, in particular TLR7, by endogenous, self-derived nucleic acids, resulting in the activation of immune cells, including primarily plasmacytoid dendritic cells (pDCs) and B cells.[8–11] These cells critically contribute to the development of the disease by producing type I interferons, proinflammatory cytokines, and autoantibodies.

Over the past decade, the endolysosomal solute carrier family 15 member 4 (SLC15A4; also known as PHT1) has emerged as a

critical component involved in TLR7–9-induced immune responses and in autoimmune diseases, a role strongly supported by both human genetics and animal studies. Indeed, evidence from genome-wide association studies (GWASs) implicated SLC15A4 in SLE.[12–17] The link between SLC15A4 and endosomal TLR7–9 responses was first revealed in an in vivo N-ethyl-N-nitrosourea (ENU) mutagenesis screen assessing serum levels of type I interferons (IFNs) upon injection of TLR7–9 agonists, which was impaired in Slc15a4-mutant feeble animals.[18] The requirement of this solute carrier for TLR7–9 function has been further established using conventional Slc15a4−/− mice and by investigating different infections and autoimmune disease models, including chemically and genetically induced SLE.[19–26] These studies demonstrated that SLC15A4 deficiency impairs TLR7–9-induced responses in multiple cell types, comprising pDCs and B cells, and confers significant protection to autoimmune diseases in vivo. Interestingly, beside TLR signaling, SLC15A4 has been implicated in other innate immune pathways, including NOD1-2 responses and inflammasome activation, and Slc15a4 deficiency has been shown to be protective also in DSS-induced colitis models.[24,27–30] Altogether, these studies support pharmacological inhibition of SLC15A4 as a potential therapeutic strategy for SLE and, possibly, other autoimmune and inflammatory conditions.
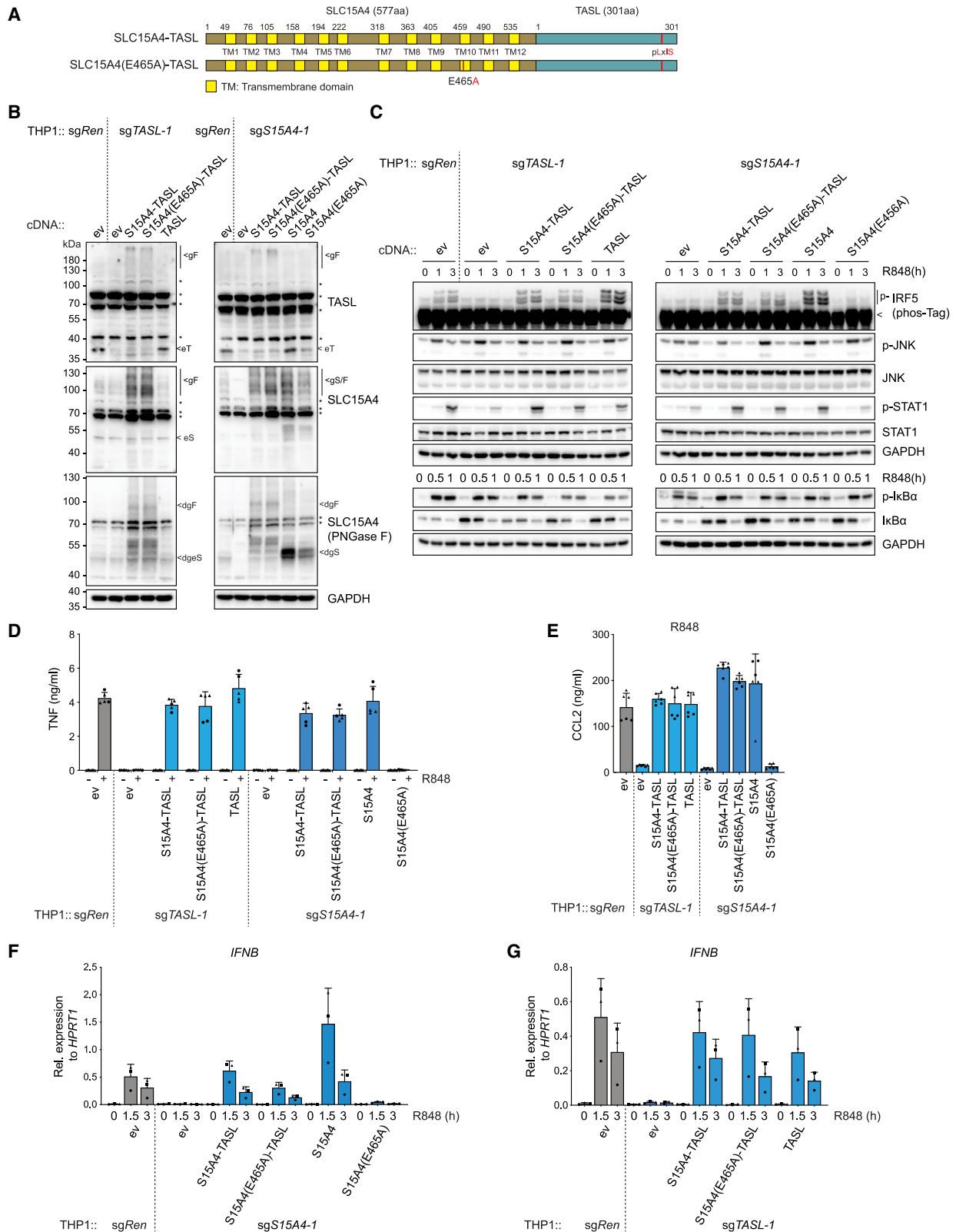
Despite these findings, the mechanism(s) by which SLC15A4 affects TLR7–9 responses remains less clear, and multiple explanations have been proposed. The SLC15 family comprises five members (1–5), and the best characterized, SLC15A1 (PepT1) and SLC15A2 (PepT2), act as plasma membrane proton-coupled oligopeptide transporters.[31] Similarly, SLC15A4 has been described as an endolysosomal proton-coupled transporter mediating histidine/oligopeptide translocation from the lumen to the cytosol.[21,30,32–34] Based on this function, SLC15A4 deficiency has been proposed to impair TLR7–9 function by altering endolysosomal homeostasis, pH, and/or histidine concentration, thereby influencing TLR maturation, TLR-ligand engagement, mTORC1 activity, or cellular metabolic processes.[18,21,24,33,35,36] Furthermore, it was recently suggested that SLC15A4 deficiency compromises the trafficking of TLRs and their ligands to endolysosomes, leading to defects in receptor engagement and in the generation of an endolysosomal organelle required for efficient signaling.[23]

Investigating this critical mechanistic aspect, we recently uncovered that SLC15A4 forms a signaling complex with a previously uncharacterized protein encoded on chromosome X by the SLE-associated gene *CXorf21*, which we named TASL.[37,38] Loss of TASL or mutations impairing complex formation phenocopied SLC15A4 deficiency, resulting in compromised type I IFN and proinflammatory cytokine production upon TLR7–9 stimulation.[37] Importantly, both SLC15A4 and TASL knockout specifically impaired TLR7–9-induced IRF5 activation without affecting the nuclear factor κB (NF-κB) and MAPK pathways, strongly suggesting that TLR-ligand engagement still occurs in SLC15A4- and TASL-deficient cells and that this complex specifically affects TLR signaling downstream of this initiating event. In line with this, we identified in the C-terminal region of TASL a pLxIS motif, which in the IRF3-adaptor proteins MAVS, STING, and TRIF is required for IRF3 recruitment and activation.[39] Analogously, the TASL pLxIS motif was essential for IRF5 binding, phosphorylation, and downstream transcriptional responses.[37] Altogether, our study revealed that SLC15A4 controls IRF5 activation by mediating the recruitment to the endolysosomal compartment of TASL, which, through its pLxIS motif, acts as a novel IRF5-activating immune adaptor.[37]

Collectively, these studies raise the question of the relative contribution for endolysosomal TLR7–9 responses of the two proposed functions of SLC15A4, i.e., transporter and TASL-recruiting signaling complex. Indeed, our data showed that the transport-inactivating mutations E465 K/A, previously used to demonstrate the importance of the SLC15A4 transporter function,[21] also resulted in a complete impairment of TASL binding.[37]

A detailed mechanistic understanding of the role of SLC15A4 is key to further evaluate its potential as therapeutic target for SLE and inform efforts aiming at pharmacologically interfering with its function.

Here, we show that the critical role of SLC15A4 in endolysosomal TLR7–9 responses is to mediate lysosomal recruitment of TASL and that SLC15A4-mediated transport activity is dispensable for IRF5 activation and proinflammatory responses, at least in conditions where TASL is localized to this compartment.
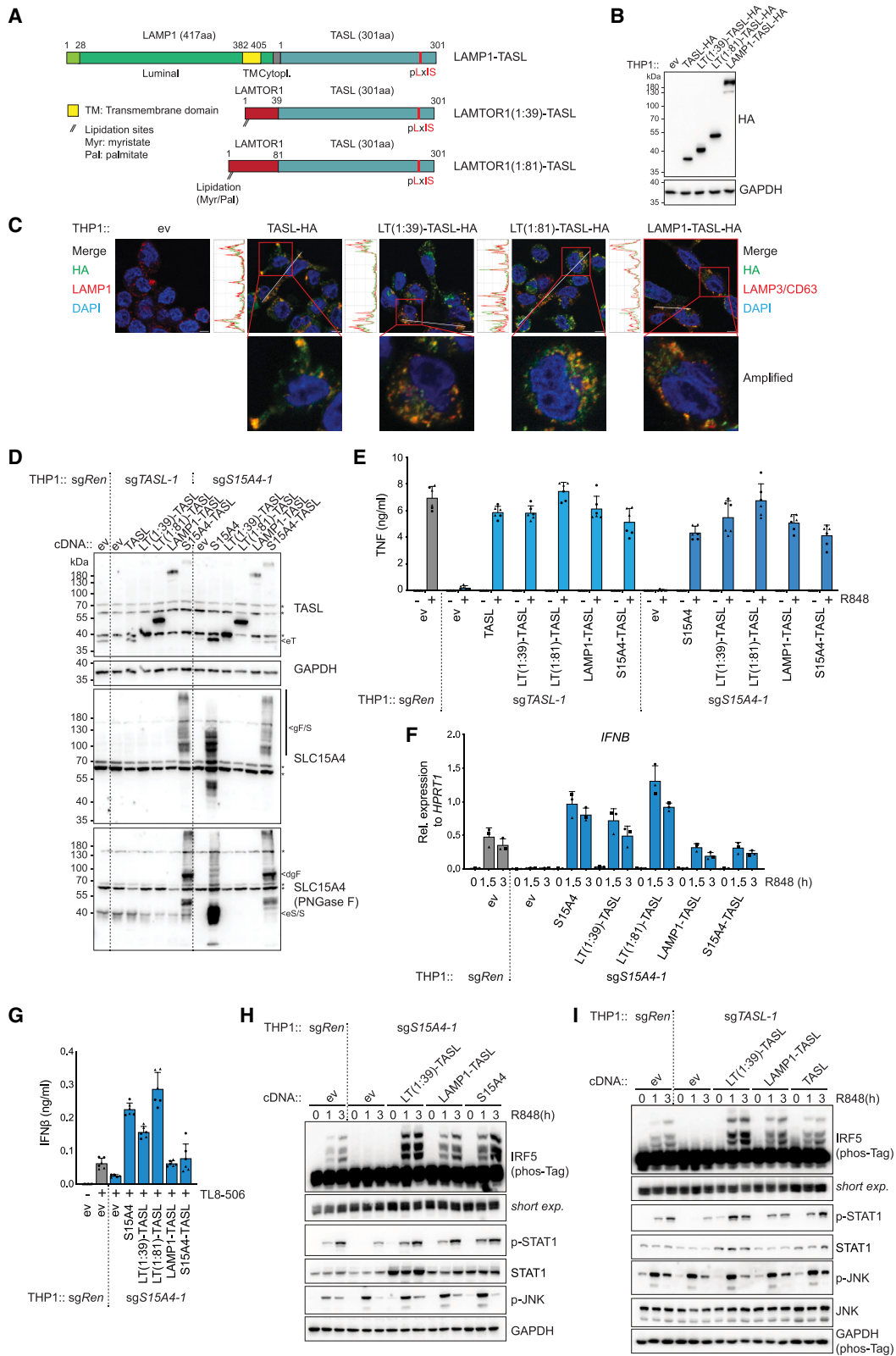
RESULTS

Fusion of TASL to transport-deficient SLC15A4(E465A) rescues TLR7/8 responses

To assess the relative contribution of SLC15A4 transport activity and endolysosomal TASL recruitment for TLR-induced responses, we devised a strategy to uncouple these two functions by fusing the TASL coding sequence to the cytoplasmic C terminus of SLC15A4, either wild type or bearing the E465A substitution (Figure 1A). Mutations of the key transmembrane residue E465 in SLC15A4 have been shown to impair both its transport function as well as TASL binding.[21,37] Accordingly, SLC15A4 E465 mutants failed to rescue TLR7–9-induced signaling when expressed in SLC15A4-deficient cells.[37] We first verified that fusion of TASL to the SLC15A4 C terminus did not alter its trafficking to the endolysosomal compartment. When stably expressed in human monocytic THP1 cells, SLC15A4-TASL and SLC15A4(E465A)-TASL fusion proteins showed the expected glycosylation, with multiple high-molecular-weight bands (130–180 kDa) detected collapsing to a single band of around 90 kDa after PNGase F treatment (Figure S1A). In line with this, both fusion proteins were detected on LAMP1- and LAMP2-positive lysosomes in these TLR7/8-signaling competent cells (Figures S1B and S1C).

Next, we stably expressed these constructs in SLC15A4- or TASL-deficient THP1 cells to assess their activity (Figure 1B). Of note, TASL protein stability depends on SLC15A4 binding,[37] resulting in the lower endogenous levels observed in SLC15A4-knockout lines. As expected, expression of wild-type SLC15A4, but not SLC15A4(E465A), in SLC15A4-knockout cells restored IRF5 activation upon stimulation with TLR7/8 agonist R848 (resiquimod), as assessed by IRF5 phosphorylation on phos-Tag-containing gels (Figure 1C). Importantly, SLC15A4-TASL and, most notably, SLC15A4(E465A)-TASL constructs fully rescued IRF5 activation in SLC15A4-deficient cells, indicating that fusion of TASL to the inactive SLC15A4(E465A) restored its functionality (Figure 1C). These data were further

Figure 1. SLC15A4 transporter activity is dispensable for TLR7/8-induced IRF5 signaling

(A) Schematic of SLC15A4-TASL and SLC15A4(E465A)-TASL fusion proteins.

(B) Immunoblots of cell lysates from THP1 carrying single guide RNAs (sgRNAs) targeting *SLC15A4* (sg*SLC15A4*-1) or *TASL* (sg*TASL*-1) or control sgRNA targeting *Renilla* (sg*Ren*) and stably expressing the indicated constructs. Where indicated, lysates were treated with PNGase F. Asterisks: unspecific bands. Arrows: specific signals. ev, empty vector; e, endogenous; g, glycosylated; dg, deglycosylated; T, TASL; S, SLC15A4; F, fusions.

(C) Immunoblots of lysates from the indicated THP1 stimulated with R848. p-, phosphorylated; phos-Tag, phos-Tag-containing gel.

(D and E) Cytokine production of indicated THP1 unstimulated or stimulated with R848.

(F and G) *IFNB* mRNA levels of indicated THP1 stimulated with R848 measured by qPCR.

(B and C) Data are representative of two independent experiments. (D and E) Mean ± SD (n = 2 biologically independent experiments performed in stimulation replicates). (F and G) Mean ± SD (n = 3 biological replicates).

See also Figures S1 and S6.

confirmed by monitoring IRF5 phosphorylation and dimerization upon stimulation with the TLR8-specific agonist TL8-506 (Figures S1D and S1E). Similar results were obtained when we assessed these constructs in TASL-knockout THP1 cells, with both SLC15A4-TASL and SLC15A4(E465A)-TASL supporting TLR7/8-induced IRF5 activation (Figure 1C). Activation of STAT1, likely resulting from IFN paracrine signaling, was equally restored by SLC15A4-TASL fusion proteins (Figure 1C). Finally, NF-κB and MAPK pathway activation, monitored by IκBα and JNK phosphorylation, respectively, proceeded independently of SLC15A4 and TASL, confirming that this complex acts downstream of TLR-ligand engagement to specifically control the IRF5 signaling branch (Figure 1C).

Next, we investigated whether SLC15A4-TASL and, in particular, SLC15A4(E465A)-TASL fusions retained the full spectrum of SLC15A4 and TASL activities by assessing the effect on downstream inflammatory cytokine and chemokine production. Expression of SLC15A4-TASL and SLC15A4(E465A)-TASL rescued both tumor necrosis factor (TNF) and C-C motif chemokine 2 (CCL2) production in SLC15A4-deficient THP1, while SLC15A4(E465A) had no effect as expected (Figures 1D and 1E). In line with this (and correlating with STAT1 activation), *IFNB* induction upon R848 stimulation was restored in SLC15A4 knockouts expressing either SLC15A4-TASL or SLC15A4(E465A)-TASL but not SLC15A4(E465A) (Figure 1F). Interestingly, both SLC15A4-TASL fusions normalized cytokine/chemokine production and *IFNB* induction also in TASL-knockout cells, suggesting that TASL does not need to be released from the endolysosomal compartment to fulfill its function (Figures 1D, 1E, and 1G).

Altogether, these results strongly suggest that SLC15A4 transport activity is not essential for TLR7/8-induced IRF5 activation and downstream signaling when TASL is tethered to endolysosomes. Rather, they support the notion that the crucial role of this solute carrier in the endolysosomal TLR pathway is to act as a signaling complex mediating the recruitment of TASL to this compartment.

Endolysosomal targeted TASL sustains TLR7/8-induced IRF5 activation independently of SLC15A4

These findings raised the question of whether endolysosomal TASL localization is in itself sufficient to mediate TLR7/8-induced IRF5 activation independently of any other possible SLC15A4 function(s). To assess this, we targeted TASL to the lysosomal compartment independently of SLC15A4 by generating fusion constructs with LAMP1 or LAMTOR1, the lysosomal-anchoring

component of the Ragulator complex (Figure 2A).[40] We selected these two lysosomal proteins because they allow anchoring of TASL to this compartment using a different mechanism than the multitransmembrane SLC15A4. In the case of LAMP1, the TASL sequence was inserted after the short, 12-amino-acid-long cytoplasmic sequence that follows its single transmembrane domain. In contrast, LAMTOR1 does not contain any transmembrane domain, and its lysosomal localization is mediated by N-terminal lipidation (myristoylation of Gly2 and palmitoylation of Cys3 and Cys4).[40] The LAMTOR1 N terminus has been previously shown to be sufficient for lysosomal localization. We therefore generated two different TASL fusion constructs, containing the first 1–39 or 1–81 amino acids of LAMTOR1.[40] Of note, both constructs do not contain the LAMTOR1 region required for binding to the other subunits of the Ragulator complex (LAMTOR2–5), therefore minimizing any risk of interfering with its functions.[40–42] Upon stable expression in THP1 cells, LAMP1-TASL and LAMTOR1-TASL fusions were targeted to the lysosomal compartment, showing partial colocalization with LAMP1, LAMP2, and/or LAMP3/CD63 markers (Figures 2B, 2C, and S2A–S2C). We have previously shown that the first N-terminal amino acids of TASL are required for SLC15A4 binding and that TASL N-terminal tagging impaired complex formation.[37] Therefore, we first investigated whether fusion of the lysosomal targeting proteins to the TASL N terminus would affect SLC15A4 binding. Indeed, TASL fusions failed to coimmunoprecipitate SLC15A4 when coexpressed in HEK293T cells (Figure S3A). In line with this, immunoprecipitation of TASL fusion proteins stably expressed in THP1 cells did not recover endogenous SLC15A4 (Figure S3B). Altogether, these results indicate that LAMTOR1- and LAMP1-TASL localized to the lysosomal compartment independently of SLC15A4.

Next, we stably expressed these fusion constructs in SLC15A4- and TASL-deficient THP1 cells, along with SLC15A4-TASL and the respective wild-type controls (Figure 2D). Remarkably, the two LAMTOR1-TASL constructs as well as LAMP1-TASL fully normalized R848-induced TNF production in both knockout cell lines (Figure 2E). CCL2 production was equally restored (Figure S3C). Supporting these data, expression of lysosomal-localized TASL in SLC15A4-deficient cells efficiently rescued IRF5 activation, monitored by its phosphorylation and dimerization, as well as STAT1 phosphorylation and *IFNB* mRNA induction and protein secretion (Figures 2F–2H and S3D). Consistently, LAMTOR1- and LAMP1-TASL efficiently complemented TLR7/8 signaling also in TASL-knockout cells (Figure 2I). Of note, compared to control sgRNA targeting *Renilla*

Figure 2. Endolysosomal-targeted TASL rescues TLR7/8-induced IRF5 signaling independently of SLC15A4
(A) Schematic of LAMP1-TASL, LAMTOR1(1:39)-TASL, and LAMTOR1(1:81)-TASL fusions.
(B) Immunoblots of THP1 stably expressing the indicated C-terminal hemagglutinin (HA)-tagged TASL fusions.
(C) Confocal microscopy of indicated THP1. Green: anti-HA; red: anti-LAMP1 or anti-LAMP3/CD63; blue: DAPI. Scale bar: 5 μm.
(D) Immunoblots of lysates from knockout THP1 stably reconstituted with indicated constructs.
(E) TNF production of indicated THP1 unstimulated or stimulated with R848.
(F) *IFNB* mRNA levels of indicated THP1 stimulated with R848 by qPCR.
(G) IFNβ production of indicated THP1 unstimulated or stimulated with TL8-506.
(H and I) Immunoblots of lysates from indicated THP1 stimulated with R848.
(B, D, H, and I) Data are representative of two independent experiments. (E and G) Mean ± SD (n = 2 biologically independent experiments performed in stimulation replicates). (F) Mean ± SD (n = 3 biological replicates).
See also Figures S2, S3, and S6.

(sg*Ren*) cells, lysosomal LAMTOR1-TASL fusions showed a mild increase in R848-induced IRF5 activation and IFNβ production (Figures 2G and 2H). This may be due to higher expression levels compared with endogenous TASL levels or, possibly, to its stable lysosomal association. Next, we investigated the specific requirement of lysosomal localization for TASL rescuing activity by tethering it to mitochondria or peroxisomes, organelles competent for MAVS signaling.[1] By fusing TASL to PEX3 peroxisomal- or TOM20 mitochondrial-targeting domains, we could achieve strong or partial relocalization to these organelles, respectively, but none of these constructs could rescue IRF5 activation (Figures S3E–S3G). This further confirms that endolysosomal localization, and not simply membrane anchoring, is essential for TASL function. To complement the data obtained upon stable expression of TASL fusion constructs, we generated SLC15A4-deficient cells inducibly expressing LAMTOR1(1:39)-TASL upon doxycycline treatment, which allowed tthe transient expression of this construct to levels comparable with endogenous TASL protein (Figure S3H). LAMTOR1(1:39)-TASL restored IRF5 activation also in these conditions, indicating that lysosomal targeting of TASL in the absence of SLC15A4 can achieve comparable activity to the endogenous protein in wild-type cells (Figure S3H). Altogether, these results reveal that the key function of SLC15A4 essential for TLR7/8-induced responses is its ability to recruit TASL to endolysosomes, as tethering of TASL to this compartment is sufficient to fully restore IRF5 activation and downstream cytokine, chemokine, and IFNβ production in SLC15A4-deficient cells. Therefore, SLC15A4-mediated transport and/or other direct or indirect metabolic effects appear to be dispensable for TLR7/8-induced IRF5-dependent responses, at least in these conditions.

Endolysosomal-tethered TASL restores TLR7–9 responses in SLC15A4-deficient pDCs and B cells

To further confirm these findings, assess possible cell-type-specific effects, and explore TLR9-induced responses, we next investigated the human pDC line CAL-1.[43] pDCs are major producers of type I IFN production upon endolysosomal TLR stimulation by microbial or endogenous nucleic acids and play a central role in SLE pathogenesis.[8,44] Moreover, CAL-1 cells express TLR9, and we previously showed that stimulation with its ligand CpG triggers SLC15A4- and TASL-dependent IRF5 activation, therefore allowing an extension of our investigation beyond TLR7/8.[37] Consistent with the data obtained in THP1 monocytes, stable expression of LAMTOR1-, LAMP1-, and SLC15A4-TASL fusion constructs restored R848-induced IRF5 activation as well as TNF and interleukin-6 (IL-6) production in both SLC15A4-and TASL-deficient CAL-1 cells (Figures 3A–3D and S4A–S4C). As we previously observed in THP1 cells,[37] deletion of TASL N-terminal residues, which mediate SLC15A4 binding, abolished activity in both TASL- and SLC15A4-deficient CAL-1 cells (Figures 3E–3G). Mitochondrial- and peroxisomal-tethered TASL were similarly inactive (Figure S4D). Furthermore, overexpression of full-length, wild-type TASL in SLC15A4-knockout cells was unable to restore IRF5 activation, confirming that lysosomal anchoring, and not increased TASL expression levels, is crucial for restoring signaling upon loss of this solute carrier (Figure S4E). In line

with THP1 data, endolysosomal-tethered LAMTOR1-TASL rescued R848-induced IFNβ production in SLC15A4-deficient cells, resulting in even higher levels than in control sg*Ren* cells, as monitored at the mRNA and protein level, as well as downstream STAT1 phosphorylation (Figures 3B, 3C, 3H, and 3I).

Importantly, the capacity of lysosomal-targeted TASL to rescue IRF5 activation in absence of SLC15A4 was not specific to TLR7/8 but was also observed upon TLR9 stimulation. Indeed, the impaired IRF5 activation observed in SLC15A4- or TASL-knockout CAL-1 upon stimulation with TLR9 agonist CpG was largely restored by expression of lysosomal TASL fusion proteins (Figures 3J, 3K, S4F, and S4G). Similar effects were observed when monitoring STAT1 activation, while, as expected, the MAPK pathway proceeded independently of the SLC15A4-TASL complex, confirming unaltered TLR-ligand engagement (Figures 3J, 3K, S4F,and S4G). Mirroring IRF5 activation, TNF and IL-6 production upon CpG was efficiently rescued by lysosomal TASL in both CAL-1 knockout lines (Figures 3L and S4H), and LAMTOR1(1:39)-TASL sustained IFNβ production in the absence of SLC15A4 also downstream of TLR9 activation (Figure S4I).

Next, we took advantage of the fact that lysosomal TASL fusions allow us to uncouple localization and signaling activity to identify domains in TASL specifically required for IRF5 activation. For this, we expressed a series of TASL-deletion constructs bearing the lysosomal LAMTOR1(1:39)-targeting motif in SLC15A4-deficient cells (Figures 3M, 3N, and S4J). Interestingly, while lysosomal TASL deleted of amino acids 1–105 retained full activity, further removal of the following evolutionary conserved region (amino acids 106–144) resulted in a complete loss of IRF5 phosphorylation, suggesting a third functional motif in TASL in addition to the N-terminal lysosomal-targeting region and the C-terminal IRF5-recruiting pLxIS motif.

Besides pDCs, B cells are key contributors to autoimmune disease pathogenesis.[9,45] In this context, accumulating evidence support a central role of cell-intrinsic endolysosomal TLR signaling in promoting the main processes by which B cells contribute to autoimmune diseases, including production of autoantibodies, antigen presentation to T cells, and production of cytokines.[9,11] *Slc15a4* deficiency in B cells affects their function and confers protection in murine SLE models,[21,25,26] but the role of this solute carrier in human B cells has not yet been investigated. Moreover, the function of TASL has not been explored in either murine or human B cells. We therefore assessed the involvement of the SLC15A4-TASL complex for endolysosomal TLR responses and IRF5 activation in Epstein–Barr virus (EBV)-immortalized human B cell lines. After verifying that R848 stimulation triggered IRF5 activation in two independent lines, we generated SLC15A4 and TASL knockouts (Figures S5A and S5B). In line with previous observations in THP1 and CAL-1 cells (Figures 1B and 3A),[37] deletion of SLC15A4 resulted in a concomitant reduction in TASL protein levels, suggesting functional complex formation also in these cells (Figures S5A and S5B). Knockout of either SLC15A4 or TASL strongly impaired IRF5 phosphorylation and dimerization in both lines, with the reduction in IRF5 activation correlating with the knockout efficiency of the different sgRNAs observed in these cell populations (Figures 4A, 4B, and S5C–S5E). Lastly, we assessed
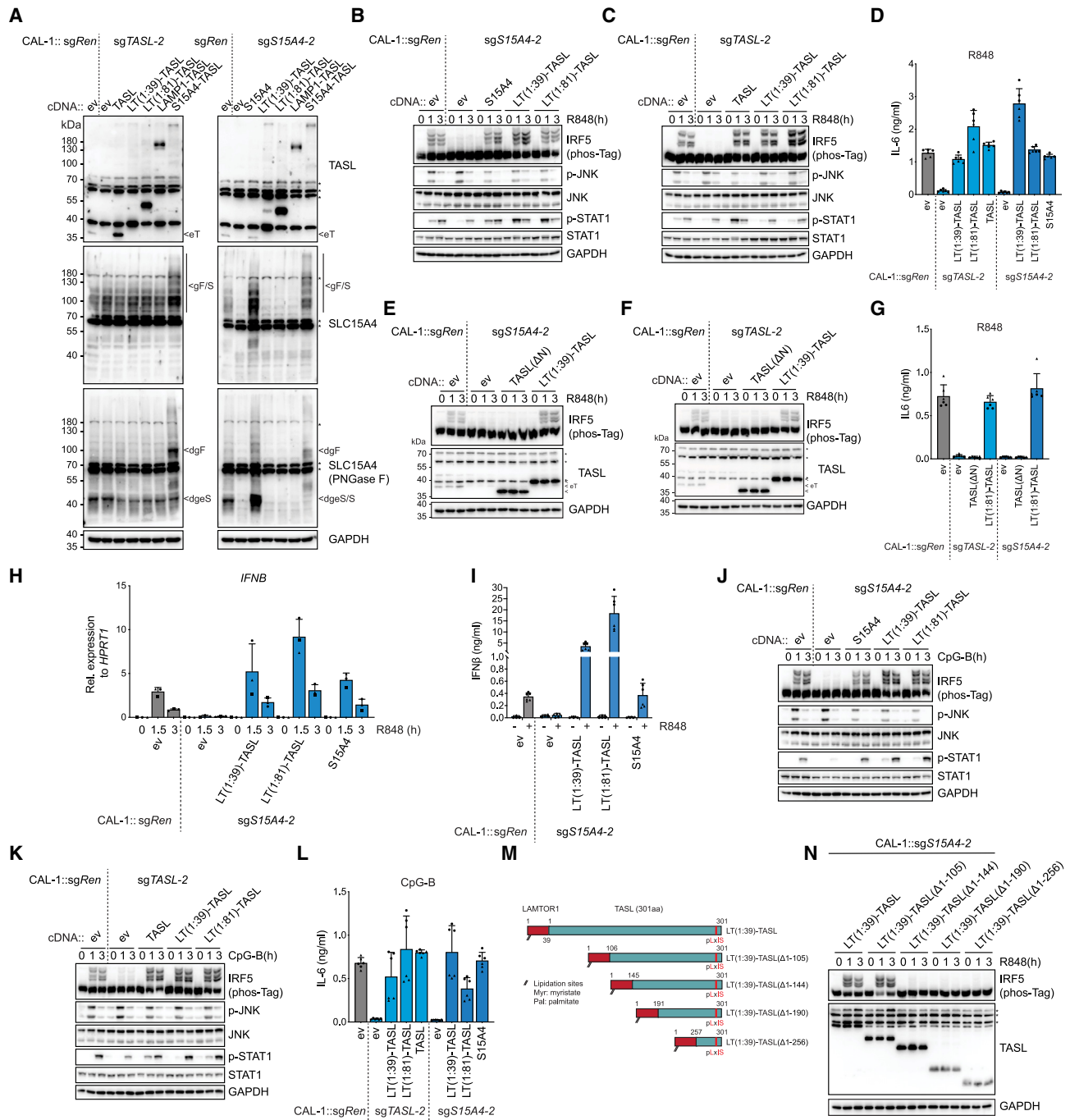
Figure 3. Endolysosomal TASL is sufficient to restore TLR7/8 and TLR9 responses in SLC15A4-deficient CAL-1 pDCs

(A) Immunoblots of knockout CAL-1 stably reconstituted with indicated constructs.

(B, C, E, F, J, and K) Immunoblots of lysates from the indicated CAL-1 stimulated with R848 (B, C, E, and F) or CpG-B (J and K).

(D, G, and L) IL-6 production of indicated CAL-1 stimulated with R848 (D and G) or CpG-B (L).

(H) *IFNB* mRNA levels of indicated CAL-1 stimulated with R848 by qPCR.

(I) IFNβ secretion of indicated CAL-1 unstimulated or stimulated with R848.

(M) Schematic of LAMTOR1(1:39)-TASL deletions.

(N) Immunoblots of indicated CAL-1 stimulated with R848.

(A–C, E, F, J, K, and N) Data are representative of two independent experiments. (D, G, I, and L) Mean ± SD (n = 2 biologically independent experiments performed in stimulation replicates). (H) Mean ± SD (n = 3 biological replicates).

See also Figures S4 and S6.
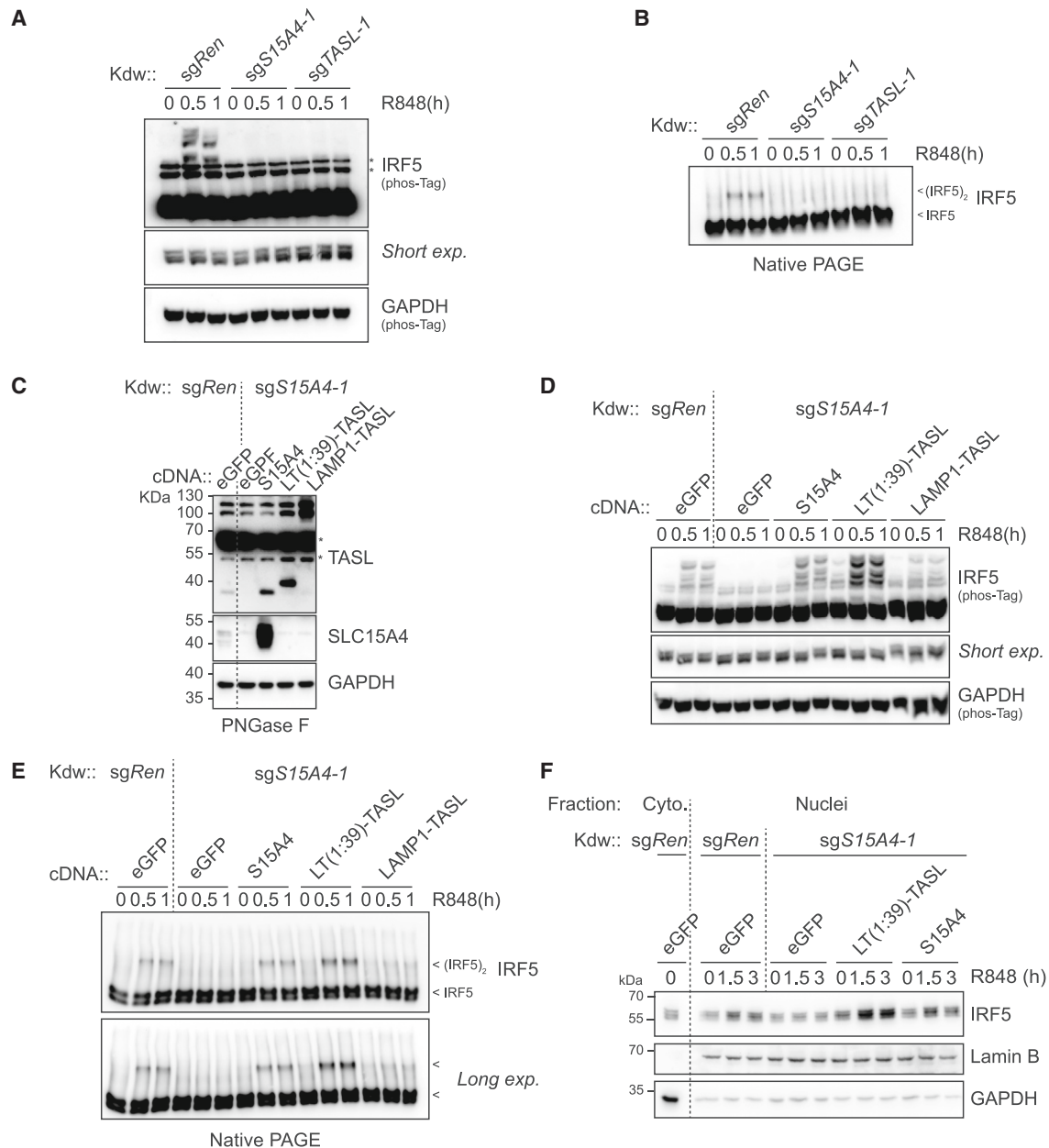
Figure 4. SLC15A4-TASL complex is essential for endolysosomal TLR-induced IRF5 activation in human B cells
(A) Immunoblots of indicated knockout Kdw cells stimulated with R848.
(B) Native PAGE immunoblot of IRF5 in knockout Kdw stimulated with R848. Arrows: monomer or dimer.
(C and D) Immunoblots of SLC15A4-knockout Kdw stably reconstituted with indicated constructs unstimulated (C) or R848 stimulated (D). (C) Lysates treated with PNGase F.
(E) Native PAGE immunoblots of indicated Kdw stimulated with R848.
(F) Nuclear-cytoplasm fractionation of indicated Kdw stimulated with R848.
(A–F) Data are representative of two independent experiments.
See also Figures S5 and S6.

whether lysosomal targeting of TASL in the absence of SLC15A4 was sufficient for IRF5 activation. Consistent with results obtained in monocytic and pDC cells, lysosomal-localized LAMTOR1(1:39)-TASL efficiently rescued IRF5 phosphorylation in SLC15A4-deficient B cells, with LAMP1-TASL also showing

lower but detectable effects (Figures 4C, 4D, S5F, and S5G). Consistently, this was reflected in IRF5 dimerization levels in lysosomal TASL-expressing cells (Figure 4E). LAMTOR1 (1:39)-TASL expression also restored the increase in nuclear IRF5 levels observed in SLC15A4-knockout cells upon R848

treatment (Figure 4F). These data demonstrate that the SLC15A4-TASL complex is essential for endolysosomal TLR-induced IRF5 activation also in human B cells, therefore extending its role beyond innate immune monocytes and pDCs and demonstrating its central relevance in the main TLR7–9-responding cell types. Considering the central role of both B cells and IRF5 in autoimmune conditions and SLE in particular, these results further emphasize the therapeutic potential of targeting the SLC15A4-TASL complex in these diseases.

DISCUSSION

In this study, we show that the crucial role of SLC15A4 in controlling TLR7–9-induced IRF5 activation and cytokine production is to recruit TASL, while its substrate transport activity is not required per se once TASL is located to the endolysosomal compartment.

How SLC15A4 controls endolysosomal TLR7–9 responses remained unclear, and different mechanistic explanations, not all necessarily mutually exclusive, have been proposed. Early studies support a model in which loss of SLC15A4 proton-coupled histidine/oligopeptide transport activity results in the accumulation of its substrates in the endolysosomal lumen, thereby altering pH and/or histidine levels.[18,21,24,36] This in turn would impact TLR maturation and/or ligand-receptor engagement. Altered intralysosomal environment and consequent impaired mTORC1 activation have been also proposed to influence TLR responses by affecting a feedforward loop mediating IRF7 upregulation.[21] Finally, other studies linked SLC15A4 deficiency to perturbed trafficking and colocalization of TLRs with their ligand, resulting in impaired receptor-ligand engagement,[23] or to metabolic perturbations affecting the TCA cycle, autophagy, and/or mitochondrial integrity.[33,35] The finding that engineered lysosomal targeting of TASL is sufficient to rescue TLR7–9 responses in SLC15A4-deficient cells demonstrates that translocation or altered concentrations of potential substrates of SLC15A4 are not critically involved in TLR pathway regulation, at least in terms of IRF5 activation and production of proinflammatory cytokines and type I IFNs. Importantly, this does not exclude the possibility that SLC15A4 transport activity may indirectly affect the TLR7–9 pathway by controlling TASL recruitment. Indeed, it is conceivable that transport-dependent conformational changes in SLC15A4 could impact its ability to bind TASL and, therefore, indirectly regulate IRF5 activation and downstream signaling. Whether the ability of SLC15A4 to recruit TASL is dependent on its conformation and/or its localization along the endolysosomal system is an intriguing question to be addressed in future studies.

Concerning the function of SLC15A4 as transporter, it should be noted that this solute carrier is expressed broadly, including in cell types that do not express TLR7–9, TASL, or IRF5.[37] This strongly suggests that SLC15A4 is involved in other cellular processes beside its specific TASL-recruiting function in endolysosomal TLR signaling. This is consistent with its reported function in regulating cellular metabolism, mTORC1 activation, NOD-ligand transport, and mast cell responses.[24,27–30,35,46]

The involvement of endosomal TLR responses in SLE and related diseases is strongly supported by both animal studies and human genetics. Notably, the three components of the signaling axis we described, SLC15A4, CXorf21/TASL, and IRF5, have all been identified in GWASs on human SLE, with IRF5 being one of the best-characterized and strongly associated factors.[12,13,47,48] In line with this, IRF5-deficient mice show strong protection in a broad range of SLE disease models.[49–54] This evidence and the fact that solute carriers are an eminently druggable class of proteins have put forward SLC15A4 as an attractive drug target for SLE and related diseases.[55–57] Further supporting this notion, here we show that the SLC15A4-TASL complex is essential for IRF5 activation not only in monocytes and pDCs but also in human B cells, demonstrating therefore its general requirement in the endolysosomal TLR-responding cells shown to be critically involved in SLE pathogenesis. The data presented strongly suggest that future efforts to pharmacologically target SLC15A4 should aim at interfering with SLC15A4-TASL complex function, either by direct inhibition of its assembly or, possibly, indirectly by interfering with the trafficking of the complex to the endolysosomal compartment. In contrast, our data imply that inhibition of SLC15A4 transport activity may not be in itself sufficient to inhibit endolysosomal TLR responses if this does not concomitantly result in interfering with complex formation or localization.

Finally, from the perspective of understanding the solute carrier family and its biology, our findings further highlight the fact that SLCs can have, behind their canonical role as transporters, additional, still underappreciated functions by acting as transceptor (transporter-receptor) and signaling complexes.[58,59]

Limitations of the study

To assess the contribution for TLR7–9 responses of the two described functions of SLC15A4, TASL binding and transport activity, and uncouple these two processes, our approach relies on exogenous expression of engineered lysosomal-tethered TASL constructs in SLC15A4- and TASL-deficient human cells. Expression of these engineered constructs could potentially mask fine regulatory mechanisms that could act on the SLC15A4-TASL complex at the endogenous level. Additionally, this approach is not readily transposable to unmodified cells. Thus, the finding that SLC15A4 transport activity is, per se, dispensable for TLR7–9 responses in the exogenous settings remains to be confirmed in primary cells. While our study does not provide structural information about the SLC15A4-TASL binding mode, a recent pre-print by Custodio et al. shows, by combining AlphaFold modeling and binding assay, that the N terminus of TASL intrudes in the central cavity of SLC15A4 in an inward open conformation.[60] This model predicts, therefore, that SLC15A4-TASL complex assembly is incompatible with transport, which strongly supports our findings. Lastly, our study focused on the role of SLC15A4 in endolysosomal TLR7–9 and does not address the role of its transport activity in other pathways in which it has been involved, such as NOD1/2, mTOR, and inflammasome signaling.

STAR★METHODS

Detailed methods are provided in the online version of this paper and include the following:

- KEY RESOURCES TABLE

- RESOURCE AVAILABILITY
  - Lead contact
  - Materials availability
  - Data and code availability
- EXPERIMENTAL MODEL AND STUDY PARTICIPANT DETAILS
  - Cells
  - Plasmids
- METHOD DETAILS
  - Generation of stable knockout and overexpressing cell lines by lentiviral transduction
  - Stimulation of cell with TLR ligands
  - Cell lysis and western blotting
  - Co-immunoprecipitation
  - PNGase F treatment
  - Enzyme-linked immunosorbent assay (ELISA)
  - Quantitative real-time PCR (qPCR)
  - Confocal microscopy
  - Nuclear–cytoplasm cell fractionation assay
- QUANTIFICATION AND STATISTICAL ANALYSIS
  - Statistical analysis

SUPPLEMENTAL INFORMATION

Supplemental information can be found online at https://doi.org/10.1016/j.celrep.2023.112916.

AUTHORS CONTRIBUTIONS

Conceptualization, H.Z. and M.R.; data curation, H.Z., L.B., and M.R.; formal analysis, H.Z., L.B., M.D., and M.R.; funding acquisition, M.R.; investigation, H.Z., L.B., M.D., E.H., A.D., and M.R.; methodology, H.Z., L.B., H.E., and M.R.; project administration, M.R.; resources, H.E. and M.R.; supervision, M.R.; validation, H.Z., L.B., M.D., and M.R.; visualization, H.Z., L.B., M.D., E.H., and M.R.; writing – original draft, M.R.; writing – review & editing, H.Z., L.B., M.D., E.H., A.D., H.E., and M.R.

DECLARATION OF INTERESTS

M.R. has filed patent applications related to the SLC15A4-TASL complex.

REFERENCES

1. Brubaker, S.W., Bonham, K.S., Zanoni, I., and Kagan, J.C. (2015). Innate immune pattern recognition: a cell biological perspective. Annu. Rev. Immunol. *33*, 257–290. https://doi.org/10.1146/annurev-immunol-032414-112240.

2. Bartok, E., and Hartmann, G. (2020). Immune Sensing Mechanisms that Discriminate Self from Altered Self and Foreign Nucleic Acids. Immunity *53*, 54–77. https://doi.org/10.1016/j.immuni.2020.06.014.

3. Fitzgerald, K.A., and Kagan, J.C. (2020). Toll-like Receptors and the Control of Immunity. Cell *180*, 1044–1066. https://doi.org/10.1016/j.cell.2020.02.041.

4. Ablasser, A., and Chen, Z.J. (2019). cGAS in action: Expanding roles in immunity and inflammation. Science *363*, eaat8657. https://doi.org/10.1126/science.aat8657.

5. Lind, N.A., Rael, V.E., Pestal, K., Liu, B., and Barton, G.M. (2022). Regulation of the nucleic acid-sensing Toll-like receptors. Nat. Rev. Immunol. *22*, 224–235. https://doi.org/10.1038/s41577-021-00577-0.

6. Crow, Y.J., and Stetson, D.B. (2022). The type I interferonopathies: 10 years on. Nat. Rev. Immunol. *22*, 471–483. https://doi.org/10.1038/s41577-021-00633-9.

7. Pelka, K., Shibata, T., Miyake, K., and Latz, E. (2016). Nucleic acid-sensing TLRs and autoimmunity: novel insights from structural and cell biology. Immunol. Rev. *269*, 60–75. https://doi.org/10.1111/imr.12375.

8. Tsokos, G.C., Lo, M.S., Costa Reis, P., and Sullivan, K.E. (2016). New insights into the immunopathogenesis of systemic lupus erythematosus. Nat. Rev. Rheumatol. *12*, 716–730. https://doi.org/10.1038/nrrheum.2016.186.

9. Fillatreau, S., Manfroi, B., and Dörner, T. (2021). Toll-like receptor signalling in B cells during systemic lupus erythematosus. Nat. Rev. Rheumatol. *17*, 98–108. https://doi.org/10.1038/s41584-020-00544-4.

10. Brown, G.J., Cañete, P.F., Wang, H., Medhavy, A., Bones, J., Roco, J.A., He, Y., Qin, Y., Cappello, J., Ellyard, J.I., et al. (2022). TLR7 gain-of-function genetic variation causes human lupus. Nature *605*, 349–356. https://doi.org/10.1038/s41586-022-04642-z.

11. Ma, K., Li, J., Fang, Y., and Lu, L. (2015). Roles of B Cell-Intrinsic TLR Signals in Systemic Lupus Erythematosus. Int. J. Mol. Sci. *16*, 13084–13105. https://doi.org/10.3390/ijms160613084.

12. Han, J.W., Zheng, H.F., Cui, Y., Sun, L.D., Ye, D.Q., Hu, Z., Xu, J.H., Cai, Z.M., Huang, W., Zhao, G.P., et al. (2009). Genome-wide association study in a Chinese Han population identifies nine new susceptibility loci for systemic lupus erythematosus. Nat. Genet. *41*, 1234–1237. https://doi.org/10.1038/ng.472.

13. Bentham, J., Morris, D.L., Graham, D.S.C., Pinder, C.L., Tombleson, P., Behrens, T.W., Martín, J., Fairfax, B.P., Knight, J.C., Chen, L., et al. (2015). Genetic association analyses implicate aberrant regulation of innate and adaptive immunity genes in the pathogenesis of systemic lupus erythematosus. Nat. Genet. *47*, 1457–1464. https://doi.org/10.1038/ng.3434.

14. Langefeld, C.D., Ainsworth, H.C., Cunninghame Graham, D.S., Kelly, J.A., Comeau, M.E., Marion, M.C., Howard, T.D., Ramos, P.S., Croker, J.A., Morris, D.L., et al. (2017). Transancestral mapping and genetic load in systemic lupus erythematosus. Nat. Commun. *8*, 16021. https://doi.org/10.1038/ncomms16021.

15. Wang, C., Ahlford, A., Järvinen, T.M., Nordmark, G., Eloranta, M.L., Gunnarsson, I., Svenungsson, E., Padyukov, L., Sturfelt, G., Jönsen, A., et al. (2013). Genes identified in Asian SLE GWASs are also associated with SLE in Caucasian populations. Eur. J. Hum. Genet. *21*, 994–999. https://doi.org/10.1038/ejhg.2012.277.

16. Yin, X., Kim, K., Suetsugu, H., Bang, S.Y., Wen, L., Koido, M., Ha, E., Liu, L., Sakamoto, Y., Jo, S., et al. (2021). Meta-analysis of 208370 East Asians identifies 113 susceptibility loci for systemic lupus erythematosus. Ann. Rheum. Dis. *80*, 632–640. https://doi.org/10.1136/annrheumdis-2020-219209.

17. Lee, H.S., Kim, T., Bang, S.Y., Na, Y.J., Kim, I., Kim, K., Kim, J.H., Chung, Y.J., Shin, H.D., Kang, Y.M., et al. (2014). Ethnic specificity of lupus-associated loci identified in a genome-wide association study in Korean

women. Ann. Rheum. Dis. *73*, 1240–1245. https://doi.org/10.1136/annr-heumdis-2012-202675.

18. Blasius, A.L., Arnold, C.N., Georgel, P., Rutschmann, S., Xia, Y., Lin, P., Ross, C., Li, X., Smart, N.G., and Beutler, B. (2010). Slc15a4, AP-3, and Hermansky-Pudlak syndrome proteins are required for Toll-like receptor signaling in plasmacytoid dendritic cells. Proc. Natl. Acad. Sci. USA *107*, 19973–19978. https://doi.org/10.1073/pnas.1014051107.

19. Baccala, R., Gonzalez-Quintial, R., Blasius, A.L., Rimann, I., Ozato, K., Kono, D.H., Beutler, B., and Theofilopoulos, A.N. (2013). Essential require-ment for IRF8 and SLC15A4 implicates plasmacytoid dendritic cells in the pathogenesis of lupus. Proc. Natl. Acad. Sci. USA *110*, 2940–2945. https://doi.org/10.1073/pnas.1222798110.

20. Blasius, A.L., Krebs, P., Sullivan, B.M., Oldstone, M.B., and Popkin, D.L. (2012). Slc15a4, a gene required for pDC sensing of TLR ligands, is required to control persistent viral infection. PLoS Pathog. *8*, e1002915. https://doi.org/10.1371/journal.ppat.1002915.

21. Kobayashi, T., Shimabukuro-Demoto, S., Yoshida-Sugitani, R., Fur-uyama-Tanaka, K., Karyu, H., Sugiura, Y., Shimizu, Y., Hosaka, T., Goto, M., Kato, N., et al. (2014). The histidine transporter SLC15A4 coordinates mTOR-dependent inflammatory responses and pathogenic antibody pro-duction. Immunity *41*, 375–388. https://doi.org/10.1016/j.immuni.2014.08.011.

22. Pollard, K.M., Escalante, G.M., Huang, H., Haraldsson, K.M., Hultman, P., Christy, J.M., Pawar, R.D., Mayeux, J.M., Gonzalez-Quintial, R., Baccala, R., et al. (2017). Induction of Systemic Autoimmunity by a Xenobiotic Re-quires Endosomal TLR Trafficking and Signaling from the Late Endosome and Endolysosome but Not Type I IFN. J. Immunol. *199*, 3739–3747. https://doi.org/10.4049/jimmunol.1700332.

23. Rimann, I., Gonzalez-Quintial, R., Baccala, R., Kiosses, W.B., Teijaro, J.R., Parker, C.G., Li, X., Beutler, B., Kono, D.H., and Theofilopoulos, A.N. (2022). The solute carrier SLC15A4 is required for optimal trafficking of nu-cleic acid-sensing TLRs and ligands to endolysosomes. Proc. Natl. Acad. Sci. USA *119*, e2200544119. https://doi.org/10.1073/pnas.2200544119.

24. Sasawatari, S., Okamura, T., Kasumi, E., Tanaka-Furuyama, K., Yanobu-Takanashi, R., Shirasawa, S., Kato, N., and Toyama-Sorimachi, N. (2011). The solute carrier family 15A4 regulates TLR9 and NOD1 functions in the innate immune system and promotes colitis in mice. Gastroenterology *140*, 1513–1525. https://doi.org/10.1053/j.gastro.2011.01.041.

25. Dosenovic, P., Ádori, M., Adams, W.C., Pedersen, G.K., Soldemo, M., Beutler, B., and Karlsson Hedestam, G.B. (2015). Slc15a4 function is required for intact class switch recombination to IgG2c in response to TLR9 stimulation. Immunol. Cell Biol. *93*, 136–146. https://doi.org/10.1038/icb.2014.82.

26. Katewa, A., Suto, E., Hui, J., Heredia, J., Liang, J., Hackney, J., Anderson, K., Alcantar, T.M., Bacarro, N., Dunlap, D., et al. (2021). The peptide sym-porter SLC15A4 is essential for the development of systemic lupus erythe-matosus in murine models. PLoS One *16*, e0244439. https://doi.org/10.1371/journal.pone.0244439.

27. López-Haber, C., Netting, D.J., Hutchins, Z., Ma, X., Hamilton, K.E., and Mantegazza, A.R. (2022). The phagosomal solute transporter SLC15A4 promotes inflammasome activity via mTORC1 signaling and autophagy restraint in dendritic cells. EMBO J. *41*, e111161. https://doi.org/10.15252/embj.2022111161.

28. Nakamura, N., Lill, J.R., Phung, Q., Jiang, Z., Bakalarski, C., de Mazière, A., Klumperman, J., Schlatter, M., Delamarre, L., and Mellman, I. (2014). Endosomes are specialized platforms for bacterial sensing and NOD2 sig-nalling. Nature *509*, 240–244. https://doi.org/10.1038/nature13133.

29. Lee, J., Tattoli, I., Wojtal, K.A., Vavricka, S.R., Philpott, D.J., and Girardin, S.E. (2009). pH-dependent internalization of muramyl peptides from early endosomes enables Nod1 and Nod2 signaling. J. Biol. Chem. *284*, 23818–23829. https://doi.org/10.1074/jbc.M109.033670.

30. Hu, Y., Song, F., Jiang, H., Nuñez, G., and Smith, D.E. (2018). SLC15A2 and SLC15A4 Mediate the Transport of Bacterially Derived Di/Tripeptides To Enhance the Nucleotide-Binding Oligomerization

Domain-Dependent Immune Response in Mouse Bone Marrow-Derived Macrophages. J. Immunol. *201*, 652–662. https://doi.org/10.4049/jimmu-nol.1800210.

31. Newstead, S. (2017). Recent advances in understanding proton coupled peptide transport via the POT family. Curr. Opin. Struct. Biol. *45*, 17–24. https://doi.org/10.1016/j.sbi.2016.10.018.

32. Yamashita, T., Shimada, S., Guo, W., Sato, K., Kohmura, E., Hayakawa, T., Takagi, T., and Tohyama, M. (1997). Cloning and functional expression of a brain peptide/histidine transporter. J. Biol. Chem. *272*, 10205–10211. https://doi.org/10.1074/jbc.272.15.10205.

33. Kobayashi, T., Nguyen-Tien, D., Ohshima, D., Karyu, H., Shimabukuro-Demoto, S., Yoshida-Sugitani, R., and Toyama-Sorimachi, N. (2021). Hu-man SLC15A4 is crucial for TLR-mediated type I interferon production and mitochondrial integrity. Int. Immunol. *33*, 399–406. https://doi.org/10.1093/intimm/dxab006.

34. Wang, X.X., Hu, Y., Keep, R.F., Toyama-Sorimachi, N., and Smith, D.E. (2017). A novel role for PHT1 in the disposition of l-histidine in brain: In vitro slice and in vivo pharmacokinetic studies in wildtype and Pht1 null mice. Biochem. Pharmacol. *124*, 94–102. https://doi.org/10.1016/j.bcp.2016.11.012.

35. Kobayashi, T., Nguyen-Tien, D., Sorimachi, Y., Sugiura, Y., Suzuki, T., Karyu, H., Shimabukuro-Demoto, S., Uemura, T., Okamura, T., Taguchi, T., et al. (2021). SLC15A4 mediates M1-prone metabolic shifts in macro-phages and guards immune cells from metabolic stress. Proc. Natl. Acad. Sci. USA *118*, e2100295118. https://doi.org/10.1073/pnas.2100295118.

36. Toyama-Sorimachi, N., and Kobayashi, T. (2021). Lysosomal amino acid transporters as key players in inflammatory diseases. Int. Immunol. *33*, 853–858. https://doi.org/10.1093/intimm/dxab069.

37. Heinz, L.X., Lee, J., Kapoor, U., Kartnig, F., Sedlyarov, V., Papakostas, K., César-Razquin, A., Essletzbichler, P., Goldmann, U., Stefanovic, A., et al. (2020). TASL is the SLC15A4-associated adaptor for IRF5 activation by TLR7-9. Nature *581*, 316–322. https://doi.org/10.1038/s41586-020-2282-0.

38. Odhams, C.A., Roberts, A.L., Vester, S.K., Duarte, C.S.T., Beales, C.T., Clarke, A.J., Lindinger, S., Daffern, S.J., Zito, A., Chen, L., et al. (2019). Interferon inducible X-linked gene CXorf21 may contribute to sexual dimorphism in Systemic Lupus Erythematosus. Nat. Commun. *10*, 2164. https://doi.org/10.1038/s41467-019-10106-2.

39. Liu, S., Cai, X., Wu, J., Cong, Q., Chen, X., Li, T., Du, F., Ren, J., Wu, Y.T., Grishin, N.V., and Chen, Z.J. (2015). Phosphorylation of innate immune adaptor proteins MAVS, STING, and TRIF induces IRF3 activation. Sci-ence *347*, aaa2630. https://doi.org/10.1126/science.aaa2630.

40. Nada, S., Hondo, A., Kasai, A., Koike, M., Saito, K., Uchiyama, Y., and Okada, M. (2009). The novel lipid raft adaptor p18 controls endosome dy-namics by anchoring the MEK-ERK pathway to late endosomes. EMBO J. *28*, 477–489. https://doi.org/10.1038/emboj.2008.308.

41. de Araujo, M.E.G., Naschberger, A., Fürnrohr, B.G., Stasyk, T., Dunzen-dorfer-Matt, T., Lechner, S., Welti, S., Kremser, L., Shivalingaiah, G., Off-terdinger, M., et al. (2017). Crystal structure of the human lysosomal mTORC1 scaffold complex and its impact on signaling. Science *358*, 377–381. https://doi.org/10.1126/science.aao1583.

42. Yonehara, R., Nada, S., Nakai, T., Nakai, M., Kitamura, A., Ogawa, A., Na-katsumi, H., Nakayama, K.I., Li, S., Standley, D.M., et al. (2017). Structural basis for the assembly of the Ragulator-Rag GTPase complex. Nat. Com-mun. *8*, 1625. https://doi.org/10.1038/s41467-017-01762-3.

43. Maeda, T., Murata, K., Fukushima, T., Sugahara, K., Tsuruda, K., Anami, M., Onimaru, Y., Tsukasaki, K., Tomonaga, M., Moriuchi, R., et al. (2005). A novel plasmacytoid dendritic cell line, CAL-1, established from a patient with blastic natural killer cell lymphoma. Int. J. Hematol. *81*, 148–154. https://doi.org/10.1532/ijh97.04116.

44. Gilliet, M., Cao, W., and Liu, Y.J. (2008). Plasmacytoid dendritic cells: sensing nucleic acids in viral infection and autoimmune diseases. Nat. Rev. Immunol. *8*, 594–606. https://doi.org/10.1038/nri2358.

45. Rubin, S.J.S., Bloom, M.S., and Robinson, W.H. (2019). B cell checkpoints in autoimmune rheumatic diseases. Nat. Rev. Rheumatol. *15*, 303–315. https://doi.org/10.1038/s41584-019-0211-0.

46. Kobayashi, T., Tsutsui, H., Shimabukuro-Demoto, S., Yoshida-Sugitani, R., Karyu, H., Furuyama-Tanaka, K., Ohshima, D., Kato, N., Okamura, T., and Toyama-Sorimachi, N. (2017). Lysosome biogenesis regulated by the amino-acid transporter SLC15A4 is critical for functional integrity of mast cells. Int. Immunol. *29*, 551–566. https://doi.org/10.1093/intimm/dxx063.

47. Graham, R.R., Kozyrev, S.V., Baechler, E.C., Reddy, M.V.P.L., Plenge, R.M., Bauer, J.W., Ortmann, W.A., Koeuth, T., González Escribano, M.F., et al.; Argentine and Spanish Collaborative Groups (2006). A common haplotype of interferon regulatory factor 5 (IRF5) regulates splicing and expression and is associated with increased risk of systemic lupus erythematosus. Nat. Genet. *38*, 550–555. https://doi.org/10.1038/ng1782.

48. Sigurdsson, S., Nordmark, G., Göring, H.H.H., Lindroos, K., Wiman, A.C., Sturfelt, G., Jönsen, A., Rantapää-Dahlqvist, S., Möller, B., Kere, J., et al. (2005). Polymorphisms in the tyrosine kinase 2 and interferon regulatory factor 5 genes are associated with systemic lupus erythematosus. Am. J. Hum. Genet. *76*, 528–537. https://doi.org/10.1086/428480.

49. Richez, C., Yasuda, K., Bonegio, R.G., Watkins, A.A., Aprahamian, T., Busto, P., Richards, R.J., Liu, C.L., Cheung, R., Utz, P.J., et al. (2010). IFN regulatory factor 5 is required for disease development in the FcgammaRIIB-/-Yaa and FcgammaRIIB-/- mouse models of systemic lupus erythematosus. J. Immunol. *184*, 796–806. https://doi.org/10.4049/jimmunol.0901748.

50. Savitsky, D.A., Yanai, H., Tamura, T., Taniguchi, T., and Honda, K. (2010). Contribution of IRF5 in B cells to the development of murine SLE-like disease through its transcriptional control of the IgG2a locus. Proc. Natl. Acad. Sci. USA *107*, 10154–10159. https://doi.org/10.1073/pnas.1005599107.

51. Tada, Y., Kondo, S., Aoki, S., Koarada, S., Inoue, H., Suematsu, R., Ohta, A., Mak, T.W., and Nagasawa, K. (2011). Interferon regulatory factor 5 is critical for the development of lupus in MRL/lpr mice. Arthritis Rheum. *63*, 738–748. https://doi.org/10.1002/art.30183.

52. Feng, D., Yang, L., Bi, X., Stone, R.C., Patel, P., and Barnes, B.J. (2012). Irf5-deficient mice are protected from pristane-induced lupus via increased Th2 cytokines and altered IgG class switching. Eur. J. Immunol. *42*, 1477–1487. https://doi.org/10.1002/eji.201141642.

53. Yasuda, K., Watkins, A.A., Kochar, G.S., Wilson, G.E., Laskow, B., Richez, C., Bonegio, R.G., and Rifkin, I.R. (2014). Interferon regulatory factor-5 deficiency ameliorates disease severity in the MRL/lpr mouse model of lupus in the absence of a mutation in DOCK2. PLoS One *9*, e103478. https://doi.org/10.1371/journal.pone.0103478.

54. Ban, T., Kikuchi, M., Sato, G.R., Manabe, A., Tagata, N., Harita, K., Nishiyama, A., Nishimura, K., Yoshimi, R., Kirino, Y., et al. (2021). Genetic and chemical inhibition of IRF5 suppresses pre-existing mouse lupus-like disease. Nat. Commun. *12*, 4379. https://doi.org/10.1038/s41467-021-24609-4.

55. Casiraghi, A., Bensimon, A., and Superti-Furga, G. (2021). Recent developments in ligands and chemical probes targeting solute carrier transporters. Curr. Opin. Chem. Biol. *62*, 53–63. https://doi.org/10.1016/j.cbpa.2021.01.012.

56. Wang, W.W., Gallo, L., Jadhav, A., Hawkins, R., and Parker, C.G. (2020). The Druggability of Solute Carriers. J. Med. Chem. *63*, 3834–3867. https://doi.org/10.1021/acs.jmedchem.9b01237.

57. Lazar, D.C., Wang, W.W., Chiu, T.-Y., Li, W., Jadhav, A.M., Wozniak, J.M., Gazaniga, N., Theofilopoulos, A.N., Teijaro, J.R., and Parker, C.G. (2022). Chemoproteomics-guided development of SLC15A4 inhibitors with anti-inflammatory activity. Preprint at bioRxiv. https://doi.org/10.1101/2022.10.07.511216.

58. Diallinas, G. (2017). Transceptors as a functional link of transporters and receptors. Microb. Cell *4*, 69–73. https://doi.org/10.15698/mic2017.03.560.

59. Rebsamen, M., Pochini, L., Stasyk, T., de Araújo, M.E.G., Galluccio, M., Kandasamy, R.K., Snijder, B., Fauster, A., Rudashevskaya, E.L., Bruckner, M., et al. (2015). SLC38A9 is a component of the lysosomal amino acid sensing machinery that controls mTORC1. Nature *519*, 477–481. https://doi.org/10.1038/nature14107.

60. Custódio, T., Killer, M., Yu, D., Puente, V., Teufel, D., Pautsch, A., Schnapp, G., Grundl, M., Kosinski, J., and Loew, C. (2023). Molecular basis of TASL recruitment by PHT1. Preprint at Research Square. https://doi.org/10.21203/rs.3.rs-2646698/v1.

61. Sic, H., Kraus, H., Madl, J., Flittner, K.A., von Münchow, A.L., Pieper, K., Rizzi, M., Kienzler, A.K., Ayata, K., Rauer, S., et al. (2014). Sphingosine-1-phosphate receptors control B-cell migration through signaling components associated with primary immunodeficiencies, chronic lymphocytic leukemia, and multiple sclerosis. J. Allergy Clin. Immunol. *134*, 420–428. https://doi.org/10.1016/j.jaci.2014.01.037.

62. Vallese, F., Catoni, C., Cieri, D., Barazzuol, L., Ramirez, O., Calore, V., Bonora, M., Giamogante, F., Pinton, P., Brini, M., and Calì, T. (2020). An expanded palette of improved SPLICS reporters detects multiple organelle contacts in vitro and in vivo. Nat. Commun. *11*, 6069. https://doi.org/10.1038/s41467-020-19892-6.

63. Calì, T., and Brini, M. (2021). Quantification of organelle contact sites by split-GFP-based contact site sensors (SPLICS) in living cells. Nat. Protoc. *16*, 5287–5308. https://doi.org/10.1038/s41596-021-00614-1.

STAR★METHODS

KEY RESOURCES TABLE

REAGENT or RESOURCE	SOURCE	IDENTIFIER
Antibodies		
Custom rabbit anti-SLC15A4	Genscript, described in[37]	N/A
Custom rabbit anti-TASL	Eurogentec, this paper	N/A
Rabbit anti-SAPK/JNK	Cell Signaling	Cat# 9252; RRID: AB_2250373
Rabbit anti-phospho-SAPK/JNK	Cell Signaling	Cat# 4668; RRID: AB_823588
Rabbit anti-STAT1	Cell Signaling	Cat# 14994; RRID: AB_2737027
Rabbit anti-phospho-STAT1	Cell Signaling	Cat# 7649; RRID: AB_10950970
Mouse anti-IkBα	Cell Signaling	Cat# 4814; RRID: AB_390781
Rabbit anti-phospho-IkBα	Cell Signaling	Cat# 2859; RRID: AB_561111
Mouse anti-Flag M2	Sigma	Cat# F1804; RRID: AB_262044
Rabbit anti-TASL (CXorf21)	Sigma	Cat# HPA001185; RRID: AB_1078591
Rabbit anti-IRF5	Abcam	Cat# ab181553; RRID: AB_2801301
Mouse anti-GAPDH	Santa Cruz	Cat# sc-365062; RRID: AB_10847862
Goat anti-Lamin B	Santa Cruz	Cat# sc-6217; RRID: AB_648158
Goat anti-rabbit IgG (H + L) HRP	Jackson Immuno Research	Cat# 111-035-003; RRID: AB_2313567
Goat anti-mouse IgG (H + L) HRP	Jackson Immuno Research	Cat# 115-035-003; RRID: AB_10015289
Peroxidase-AffiniPure Donkey anti-Goat IgG (H + L)	Jackson Immuno Research	Cat# 705-035-003; RRID: AB_2340390
Rabbit anti-HA	Cell signaling	Cat# 3724; RRID: AB_1549585
Mouse anti-LAMP2	Santa Cruz	Cat# sc-18822; RRID: AB_626858
Mouse anti-LAMP1	Santa Cruz	Cat# sc-20011; RRID: AB_626853
Mouse anti-LAMP3/CD63	DHSB	Cat# h5c6; RRID: AB_528158
Mouse anti-Catalase	R&D Systems	Cat# MAB3398; RRID: N/A
Goat anti-Mouse IgG (H + L) Cross-Adsorbed Secondary Antibody, Alexa Fluor™ 594	Invitrogen	Cat# A-11005, RRID; AB_2534073
Goat anti-Rabbit IgG (H + L) Highly Cross-Adsorbed Secondary Antibody, Alexa Fluor™ 488	Invitrogen	Cat# A-11034, RRID; AB_2576217
Chemicals, peptides, and recombinant proteins		
R848	Invivogen	tlrl-r848-5
TL8-506	Invivogen	tlrl-tl8506
Doxycycline	Sigma	D9891-1G
CpG (ODN2006)	IDT	N/A
Polybrene	Sigma	H9268
EDTA-free Protease Inhibitor Cocktail	Roche	11836170001
Halt™ Phosphatase Inhibitor Cocktail	Thermo Scientific	78420
Phos-tag™ Acrylamide	Wako Chemicals	304–93521
PMA	Sigma	P8139-1MG
Formaldehyde	Sigma	F1635-50ML
Saponin	Sigma	47036-50G-F
DAPI	Invitrogen	R37606
MitoTracker Red CMXRos	Thermo Scientific	M7512
ProLong Gold	Invitrogen	P10144
Critical commercial assays		
Gibson Assembly Cloning Kit	NEB	E5510
Gateway™ BP Clonase™ II Enzyme mix	Invitrogen	11789100

Continued

REAGENT or RESOURCE	SOURCE	IDENTIFIER
TNF alpha Human Uncoated ELISA Kit	Invitrogen	88-7346-88
IL-6 Human Uncoated ELISA Kit	Invitrogen	88-7066-88
MCP-1/CCL2 Human Uncoated ELISA Kit	Invitrogen	88-7399-88
Human IFN-beta DuoSet ELISA	R & D Systems	DY814-05
RevertAid First Strand cDNA Synthesis Kit	Thermo Scientific	K1622
LightCycler® 480 SYBR Green I Master	Roche	04707516001
Experimental models: Cell lines		
HEK293T	ATCC	CRL-3216
THP1	ATCC	TIB-202
CAL-1	T.Maeda (Nagasaki University)[43]	N/A
EBV-immortalized human B cell lines (Kdw and Pdw)	this paper	N/A
Oligonucleotides		
See Table S1	IDT & Sigma	N/A
Software and algorithms		
Prism 9	GraphPad	https://www.graphpad.com
ZEN 2.3	Carl Zeiss	https://www.zeiss.com/microscopy/en/products/software/zeiss-zen.html
Fiji	ImageJ	https://imagej.net/software/fiji/
BioRender	BioRender.com	https://www.biorender.com/

RESOURCE AVAILABILITY

Lead contact
Further information and requests for resources and reagents should be directed to and will be fulfilled by the lead contact Manuele Rebsamen (manuele.rebsamen@unil.ch).

Materials availability
All unique reagents generated in this study are available from the lead contact upon completion of a Material Transfer Agreement.

Data and code availability
- All data reported in this paper will be shared by the lead contact upon request.
- This paper does not report original code.
- Any additional information required to reanalyze the data reported in this paper is available from the lead contact upon request.

EXPERIMENTAL MODEL AND STUDY PARTICIPANT DETAILS

Cells
HEK293T cells and THP1 cells were purchased from ATCC. CAL-1 cells were kindly provided by T. Maeda (Nagasaki University).[43] EBV lines (Kdw and Pdw) were obtained by immortalizing B cells of healthy donors as described in.[61] HEK293T cells were cultured in DMEM (Gibco), THP1, CAL-1 and B cells in RPMI (Gibco), supplemented with 10% (v/v) fetal bovine serum (FBS, Gibco) and anti-biotics (100 U/ml penicillin, 100 μg/mL streptomycin, Bioconcept) at 37°C in 5% CO2 incubator.

Plasmids
Codon-optimized cDNAs for human SLC15A4 and TASL have been described previously.[37] A template for cloning human LAMP1 (no. 134868) and DOX-inducible lentiviral gene expression vector pINDUCER21 (ORF-EG) (no. 46948) were from Addgene. Gateway pDONR201 plasmid LAMTOR1 has been described before.[59] Gibson assembly cloning (NEB) was used to clone endolysosomal TASL fusion constructs (SLC15A4-TASL, SLC15A4(E465A)-TASL, LAMTOR1(1:39)-TASL, LAMTOR1(1:81)-TASL and LAMP1-linker(13 aa)-TASL (referred to as LAMP1-TASL)). Point mutation SLC15A4(E465A) was introduced by site-directed mutagenesis. LAMTOR1(1:39)-TASL deletion constructs (LAMTOR1(1:39)-TASL Δ1-105, Δ1-144, Δ1-190, Δ1-256) were generated by PCR mutagenesis. C-tag or HA-tag was added to the C terminus of different TASL fusions by PCR. Tethering of TASL to peroxisomes or the outer mitochondrial membrane was achieved by fusing to its N terminus previously described targeting sequences: the first

40 N-terminal amino acids of PEX3 (PO-TASL),[62] or the first 33 N-terminal amino acids of TOM20 (MM-TASL).[63] All cDNAs were subcloned into pDONR201/221 (Invitrogen), verified by sequencing and shuttled by Gateway cloning (Invitrogen) to destination vectors: pINDUCER21 or pRRL-based lentiviral expression plasmids with a selectable resistance cassette allowing untagged, N- or C-terminal Strep-HA-tagged (SH) or V5-tagged expression.[37] CRISPR–Cas9-based knockout cell line generation was performed using pLentiCRISPRv2 (Addgene plasmid no. 52961) and sgRNA sequences targeting *SLC15A4* (sg*SLC15A4*-1 and sg*SLC15A4*-2), *TASL* (sg*TASL*-1 and sg*TASL*-2) or a non-targeting, control sgRNA sequence designed against *Renilla* (sg*Ren*) previously described (Table S1).[37]

METHOD DETAILS

Generation of stable knockout and overexpressing cell lines by lentiviral transduction

Lentiviral transduction was performed as previously described.[37] Briefly, HEK293T cells were transfected with sgRNA- or cDNA-encoding lentiviral vectors and packaging plasmids psPAX2 and pMD2.G (plasmid no. 12260 and plasmid no. 12259 from Addgene) using PEI (Sigma). The medium was changed with fresh RPMI, supplemented with 10% (v/v) fetal bovine serum (FBS) and antibiotics (100 U/ml penicillin, 100 μg/mL streptomycin) 6h post transfection. After 48h, virus-containing supernatants were harvested, filtered through 0.45-μm polyethersulfone filters (Millipore) and supplemented with 5 μg/mL polybrene (Sigma) for infection. Cells were infected by spin infection (2,000 rpm, 45 min, room temperature). 24/48h later, cells were washed and then selected with appropriate antibiotics or, in case of pINDUCER21-based vectors, sorted by FACS based on GFP signal. Selected cell populations were used for experimental investigations without further subcloning to avoid clonal effects.

Stimulation of cell with TLR ligands

If not indicated otherwise, cells were stimulated with 5μg/ml R848, 5μM CpG or 0.5 μg/mL TL8-506 for the indicated time.

Cell lysis and western blotting

Cells were lysed in RIPA (25 mM Tris, 150 mM NaCl, 0.5% NP-40, 0.5% deoxycholate (w/v), 0.1% SDS (w/v), pH 7.4) or E1A (50 mM HEPES, 250 mM NaCl, 5 mM EDTA, 1% NP-40, pH 7.4) lysis buffer. For Native-PAGE immunoblotting, cells were lysed in an NP-40 buffer (50 mM HEPES, 150 mM NaCl, 5 mM EDTA, 10% glycerol, 1% NP-40, pH 7.4). Lysis buffers were supplemented with Benzonase Nuclease (Merck), complete EDTA-free protease inhibitor cocktail (Roche) and Halt phosphatase inhibitor cocktail (Thermo Fisher Scientific). Lysates were cleared by centrifugation (13,000 rpm, 10 min, 4°C), and, after protein quantification with BCA (Thermo Fisher Scientific) using BSA as standard, resolved by regular or phos-Tag-containing (20–50 μM, WAKO Chemicals) SDS–PAGE and blotted to nitrocellulose membranes (Amersham). Prior to transfer, phos-Tag SDS-PAGE gels were incubated (2 times 10 min) with transfer buffer supplemented 10 mM EDTA and then washed 10 min in transfer buffer without EDTA. For IRF5 Native-PAGE, 10μg of lysate was separated by 7.5% polyacrylamide gel without SDS. Before transfer, gels were soaked in running buffer with 0.01% SDS for 30 min at room temperature. After transfer, membranes were blocked by 5% non-fat dry milk in TBST and probed with indicated antibodies. In experiments in which multiple antibodies were used, equal amounts of samples were loaded on multiple SDS–PAGE gels and western blots sequentially probed with a maximum of two antibodies.

Co-immunoprecipitation

For immunoprecipitation assays with tagged proteins, cells were lysed in E1A buffer. The appropriate amount of whole-cell lysate was used as input, and the remaining was subjected to immunoprecipitation using equilibrated CaptureSelect C-tagXL Affinity matrix beads (Thermo Fisher Scientific) overnight at 4°C on a rotating wheel. Beads were washed three times with E1A buffer and eluted with SDS loading buffer. Whole-cell lysate and immunoprecipitated proteins were analyzed by SDS-PAGE and immunoblotting.

PNGase F treatment

Cleared cell lysates were incubated with PNGase F (500–1,000 U per 20 μL of lysates, NEB) for 30–45 min at 37°C. Samples were analyzed by western blotting.

Enzyme-linked immunosorbent assay (ELISA)

Cells were stimulated with the indicated ligands, cell supernatants were harvested 22–24 h later and cleared from residual cells by centrifugations. Measurements of IFNβ were performed using Human IFN-beta DuoSet ELISA (R&D Systems) and undiluted supernatants according to manufacturer's instructions. All other ELISA experiments were performed using diluted supernatants according to manufacturer's instructions as described.[37]

Quantitative real-time PCR (qPCR)

Cells were collected and total RNAs were isolated using a Quick-RNA Miniprep Kit (Zymo Research). Reverse transcription was performed using RevertAid First Strand cDNA Synthesis Kit (Thermo Fisher Scientific) using oligo (dT) primers. Real-time PCR was performed using LightCycler 480 SYBR Green I Master (Roche). Gene-specific primers used are described in Table S2. Samples were

analyzed on LightCycler 480 (Roche). Data were analyzed and Ct values were calculated using LightCycler Software version 1.5 (Roche). Results were obtained using the $2^{-\Delta\Delta Ct}$ method, using HPRT1 as reference.

Confocal microscopy

These experiments were carried out as previously described.[37] In brief, 3.5×10^5 cells were seeded in 24-well plates on coverslips and treated with 10 nM PMA (Sigma) overnight to induce adherence. Cells were washed with PBS, fixed (PBS, 2% formaldehyde (Sigma)) for 20 min, permeabilized and blocked in blocking solution (PBS, 0.3% saponin (Sigma), 10% FBS) for 1 h. Afterward, cells were stained 1h at room temperature with the indicated primary antibodies in blocking solution. Antibodies or dyes used for immunofluorescence analysis in this study are rabbit anti-HA (no. 3724, Cell Signaling, 1:1,000), mouse anti-LAMP1 (sc-20011, 1:500), mouse anti-LAMP2 (sc-18822, Santa Cruz, 1:1,000), mouse anti-LAMP3/CD63 (DHSB h5c6, 1:1000), mouse anti-Catalase (R&D Systems, MAB3398, 1:500), MitoTracker Red CMXRos (M7512, Thermo Fisher Scientific). After three washes with blocking solution, cells were stained with goat anti-mouse (Alexa Fluor 594, A11005) and anti-rabbit (AlexaFlour488, A11034) antibodies (Invitrogen, 1:1,000) for 1h at room temperature. Cells were then washed once in blocking solution. Nuclear counterstaining was performed with DAPI (Invitrogen). After three washes with blocking buffer and one wash with PBS, cover glasses were mounted onto microscope slides using ProLong Gold (Invitrogen) antifade reagent. Images were acquired on a confocal laser scanning microscope (Zeiss LSM 880, Carl Zeiss) and analyzed using ZEN 2.3 (Carl Zeiss).

Nuclear-cytoplasm cell fractionation assay

Nuclear-cytoplasm cell fractionation was performed as previously described.[59] Briefly, cells were harvested, washed once with PBS and lysed in buffer N (300 mM Sucrose, 10 mM HEPES (pH 7.9), 10 mM KCl, 0.1 mM EDTA (pH 8.0), 0.1 mM EGTA (pH 7.0), 0.1 mM DTT, 0.75 mM spermidine, 0.15 mM spermine and 0.1% (w/v) NP-40) supplemented with complete EDTA-free protease inhibitor cocktail (Roche) and phosphatase inhibitor cocktail (10 mM Sodium fluoride, 2 mM Sodium pyrophosphate, 2 mM Sodium orthovanadate 400, 2 mM b-glycerophosphate). Lysates were gently vortexed, incubated on ice for 10min and centrifuged for 5 min at 500g. Supernatants containing cytoplasmic proteins were harvested in separate tubes. Nuclei pellets were washed three times with buffer N and lysed with RIPA lysis buffer (supplemented with Benzonase Nuclease (Merck), EDTA-free protease inhibitor cocktail (Roche) and Halt phosphatase inhibitor cocktail (Thermo Fisher Scientific)). Resuspended pellets were sonicated, centrifugated (10 min, 13,000 rpm, 4°C) and supernatant containing nucleic proteins were harvested.

QUANTIFICATION AND STATISTICAL ANALYSIS

Statistical analysis

Statistical analyses and graphs were made using GraphPad Prism 9 software (GraphPad). Analysis of immunofluorescence images and protein quantification were performed using Fiji. The number of experiments or biological replicates (n) used for the statistical evaluation of each experiment is indicated in the corresponding figure legends. The data are plotted as a mean ± s.d. as indicated.